



Coral records of reef-water pH across the central Great Barrier Reef, Australia: assessing the influence of river runoff on inshore reefs

J. P. D’Olivo^{1,2,3}, M. T. McCulloch^{1,2}, S. M. Eggins³, and J. Trotter²

¹The ARC Centre for Excellence for Coral Reef Studies, the University of Western Australia, Crawley 6009, Australia

²School of Earth and Environment, The University of Western Australia, Crawley 6009, Australia

³Research School of Earth Sciences, Australian National University, Canberra 0200, Australia

Correspondence to: J. P. D’Olivo (juan.dolivocordero@uwa.edu.au)
and M. T. McCulloch (malcolm.mcculloch@uwa.edu.au)

Received: 20 June 2014 – Published in Biogeosciences Discuss.: 25 July 2014

Revised: 12 January 2015 – Accepted: 22 January 2015 – Published: 25 February 2015

Abstract. The boron isotopic ($\delta^{11}\text{B}_{\text{carb}}$) compositions of long-lived *Porites* coral are used to reconstruct reef-water pH across the central Great Barrier Reef (GBR) and assess the impact of river runoff on inshore reefs. For the period from 1940 to 2009, corals from both inner- and mid-shelf sites exhibit the same overall decrease in $\delta^{11}\text{B}_{\text{carb}}$ of 0.086 ± 0.033 ‰ per decade, equivalent to a decline in seawater pH (pH_{sw}) of $\sim 0.017 \pm 0.007$ pH units per decade. This decline is consistent with the long-term effects of ocean acidification based on estimates of CO_2 uptake by surface waters due to rising atmospheric levels. We also find that, compared to the mid-shelf corals, the $\delta^{11}\text{B}_{\text{carb}}$ compositions of inner-shelf corals subject to river discharge events have higher and more variable values, and hence higher inferred pH_{sw} values. These higher $\delta^{11}\text{B}_{\text{carb}}$ values of inner-shelf corals are particularly evident during wet years, despite river waters having lower pH. The main effect of river discharge on reef-water carbonate chemistry thus appears to be from reduced aragonite saturation state and higher nutrients driving increased phytoplankton productivity, resulting in the drawdown of $p\text{CO}_2$ and increase in pH_{sw} . Increased primary production therefore has the potential to counter the more transient effects of low-pH river water (pH_{rw}) discharged into near-shore environments. Importantly, however, inshore reefs also show a consistent pattern of sharply declining coral growth that coincides with periods of high river discharge. This occurs despite these reefs having higher pH_{sw} , demonstrating the overriding importance of local reef-water quality and reduced aragonite saturation state on coral reef health.

1 Introduction

Coral reefs are under threat, not only from the global effects of CO_2 -driven climate change but also from direct local impacts, in particular disturbed river catchments and degraded water quality (McCulloch et al., 2003; Brodie et al., 2010b). Changing land-use practices since the arrival of European settlers to the central Queensland region has produced increased discharge of terrestrial material from the Burdekin River into the Great Barrier Reef (GBR; McCulloch et al., 2003; Lewis et al., 2007). The increase in discharge of terrestrial material into the GBR has resulted in a decrease in inshore water quality, mainly through increased nutrient loads and decreased water clarity (Brodie et al., 2010b; Fabricius et al., 2014). Known impacts include the promotion of intense and extensive phytoplankton blooms and the increase in abundance of macro-algae (Devlin and Brodie, 2005; Brodie et al., 2010b). Changes in water quality within inner-shelf environments of the GBR have also been linked to a decrease in coral calcification (D’Olivo et al., 2013), coral biodiversity (De’ath and Fabricius, 2010), decreased coral cover (Sweetman et al., 2011), and crown-of-thorns starfish outbreaks (Brodie et al., 2005).

Despite the mounting evidence for the negative impacts of increased terrestrial discharge into the GBR, the effect of river flood plumes on the carbonate status of reef waters, a fundamental property controlling calcification, remains largely unknown. It is commonly assumed that, because both the salinity and pH of plume waters (pH_{pw}) are

generally much lower than ocean waters, a decrease in aragonite saturation state (Ω_{arag}) might be expected (Salisbury et al., 2008), with consequent negative effects for coastal calcifying organisms such as corals (e.g., Kleypas, 1999; Doney et al., 2009; McCulloch et al., 2012). The effect of lower seawater pH (pH_{sw}) could, however, be offset by the input of nutrients associated with river plumes, as in semi-isolated environments (e.g., enclosed lagoons) and/or highly productive areas where biological processes actively modify the local seawater chemistry (e.g., Hinga, 2002; Andersson et al., 2005; Bates et al., 2010; Drupp et al., 2011; Falter et al., 2013; Duarte et al., 2013). For example, increased productivity during phytoplankton blooms can cause pH_{sw} to rise significantly (Hinga, 2002). Nutrient-enhanced photosynthetic activity has been shown to amplify the seasonal pH cycle by more than 0.5 pH units in experiments within marine enclosures in Narragansett Bay, Rhode Island (Frithsen et al., 1985), and to increase pH_{sw} by 0.7 units in the Peruvian coastal upwelling zone (Simpson and Zirino, 1980). In the GBR, it is not known to what extent terrestrial runoff and the associated phytoplankton blooms influence pH_{sw} and hence coral calcification, partly due to the sparseness of especially longer-term pH_{sw} and other seawater carbonate system records. To overcome this, here we use the skeletons of long-lived massive *Porites* corals as archives of changing environmental conditions. Temporal changes in the boron isotope ($\delta^{11}\text{B}$) composition of the skeletons provide a time series of seawater pH, which, together with instrumental data, help deconvolve the competing impacts of climate, ocean acidification, and water quality on coral calcification.

The $\delta^{11}\text{B}$ composition of biogenic carbonates ($\delta^{11}\text{B}_{\text{carb}}$) is an established paleo-proxy for pH_{sw} , first developed in corals by Vengosh et al. (1991) and Hemming and Hanson (1992) and more recently refined by Trotter et al. (2011). The method relies on the preferential incorporation of the isotopically lighter $\text{B}(\text{OH})_4^-$ over the $\text{B}(\text{OH})_3$ species into marine carbonate skeletons, with the relative boron species concentration and isotopic compositions being pH dependent (Vengosh et al., 1991; Hemming and Hanson, 1992; Hönisch et al., 2004). Its application to corals has been validated (Hönisch et al., 2004; Reynaud et al., 2004; Trotter et al., 2011) and used for long-term pH_{sw} reconstructions using massive *Porites* corals (Pelejero et al., 2005; Liu et al., 2009; Wei et al., 2009; Shinjo et al., 2013). Although coral $\delta^{11}\text{B}_{\text{carb}}$ compositions closely parallel variations in pH_{sw} (Hönisch et al., 2004; Krief et al., 2010; Trotter et al., 2011; McCulloch et al., 2012), there is a consistent species-specific positive offset of coral $\delta^{11}\text{B}_{\text{carb}}$ compositions above the borate $\delta^{11}\text{B}$ value for ambient pH_{sw} (Trotter et al., 2011; McCulloch et al., 2012). This elevation of pH was recently shown to be consistent with the physiological up-regulation of pH at the site of calcification to promote aragonite precipitation (Trotter et al., 2011; McCulloch et al., 2012). Trotter et al. (2011) quantified this internal pH offset and consequently derived ambient seawater values based on the systematic relationships

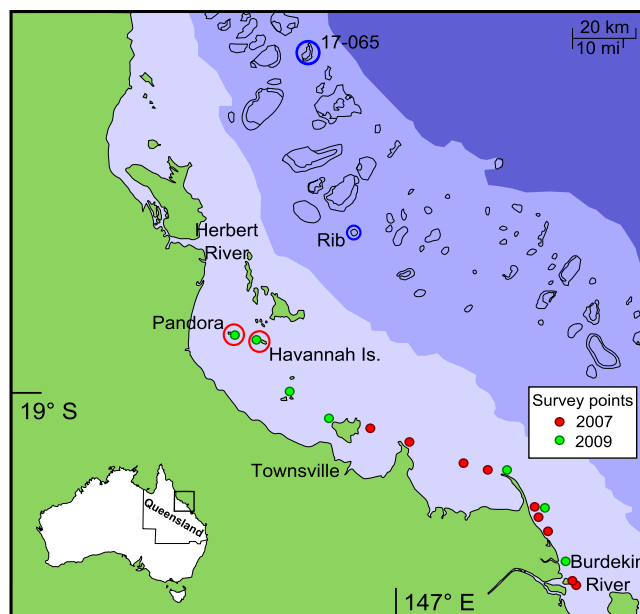


Figure 1. Map of the central area of the GBR showing locations of water sample and coral core collection sites: Pandora Reef and Havannah Island in the inner shelf, Rib Reef and 17-065 Reef in the mid-shelf region, and water sample collection sites during the flood events of 2007 and 2009.

they observed between the measured coral $\delta^{11}\text{B}_{\text{carb}}$ composition and pH_{sw} .

In this study we present annual-resolution $\delta^{11}\text{B}_{\text{carb}}$ data obtained from cores of massive *Porites* heads collected from two inner-shelf and two mid-shelf reefs of the central GBR (Fig. 1). The $\delta^{11}\text{B}_{\text{carb}}$ data are used to reconstruct the variability in surface pH_{sw} on annual timescales for the period from 1940 to 2009. These results are then compared with measurements of calcification rates (i.e., linear extension) obtained from the same cores, together with a more extensive database from the central GBR (D'Olivo et al., 2013). This sampling regime enables comparative analysis of the dynamic inner-shelf reef environments, which are subject to terrestrial and anthropogenic influences, with the more stable conditions of mid-shelf reefs that are less exposed to terrestrial runoff and pollutants (Lough, 2001; Furnas, 2003; Brodie et al., 2012). Collectively these coral records of $\delta^{11}\text{B}$ (this study) and linear extension (D'Olivo et al., 2013) provide a unique data set giving insight into the long-term variability of pH_{sw} in a natural coastal system and how these changes interrelate to other important environmental parameters (temperature, river discharge and nutrient flux) and their overall influence on coral calcification.

2 Samples and methods

2.1 Instrumental river discharge and sea surface temperature records

Monthly records of river water discharge and pH (pH_{rw}) for both the Burdekin and Herbert rivers were obtained from the State of Queensland, Department of Environment and Resource Management (DERM; <http://watermonitoring.derm.qld.gov.au>, 2011). Annual rainfall data are defined from October to September based on the rainfall seasonal pattern in Queensland, with October marking the start of the warmer summer wet season (Lough, 2007, 2011). Monthly sea surface temperature (SST) records were obtained from the Met Office Hadley Centre's sea ice and sea surface temperature data set (HadISST1) centered at 18° S and 147° E with a spatial resolution of 1° × 1° (<http://www.metoffice.gov.uk/hadobs/hadisst/>, 2014). Inner-shelf average monthly in situ SST data for the period from 1993 to 2008 were obtained from the Australian Institute of Marine Science (AIMS; <http://data.aims.gov.au/>, 2011). The inner-shelf SST data were derived by averaging temperature logger records at Pandora Reef, Havannah Island, Cleveland Bay, Pioneer Bay, Cattle Bay, and Pelorus Island (AIMS, <http://data.aims.gov.au/>, 2011).

2.2 Water samples

Water samples were collected in order to characterize the $\delta^{11}\text{B}$ composition of the plume waters ($\delta^{11}\text{B}_{\text{pw}}$) present in the inner-shelf area during flood events, and hence facilitate the interpretation of the $\delta^{11}\text{B}_{\text{carb}}$ coral signal. In February 2007, a total of 29 water samples were collected (by Stephen Lewis, James Cook University) along a northward transect from the mouth of the Burdekin River to Magnetic Island (Fig. 1). In February 2009, a second suite of water samples were collected (by J. P. D'Olivo) from the Burdekin River bridge, located between the towns of Ayr and Home Hill, as well as seven seawater samples along a northward transect from the mouth of the Burdekin River to Pandora Reef. The presence of discolored water indicated that the river plume had reached all of the sampling sites. After collection, 125 ml of each sample was filtered through a 0.45 μm Teflon membrane and then acidified using 2–3 drops of $\sim 7\text{ M HNO}_3$. Samples were then stored in acid-cleaned, low-density polyethylene bottles in a cool room. Salinity data were provided by S. Lewis (2009). Water samples were analyzed for B by solution quadrupole ICP-MS using a Varian 820 ICP-MS at the Research School of Earth Sciences at the Australian National University (ANU). ^{10}Be was used as an internal standard spiked at a concentration of 4 ppb. Water samples were diluted to a final salinity of 0.035.

2.3 Sclerochronology and coral sampling for $\delta^{11}\text{B}$ analysis

Five cores were drilled from massive Porites coral heads from four sites in the central GBR (Fig. 1): Pandora Reef (PAN02) and Havannah Island (HAV06A and HAV09_3) in the inner shelf, and Rib Reef (RIB09_3) and Reef 17-065 (1709_6) in the mid-shelf. All cores exhibit clear and regular annual growth banding. Subsamples representing annual growth increments, from the beginning of each high-density band (for mid-shelf corals) or luminescent band (for inner-shelf corals), were milled along the axis of maximum growth of 0.7 cm thick slabs from each core.

2.4 Boron isotope methodology

The boron isotopic compositions of water samples and annual coral subsamples of cores HAV06A, PAN02, and RIB03 were analyzed at the ANU by positive thermal ionization mass spectrometry (PTIMS) using a Thermo Finnigan TRITON. Annual coral subsamples of cores HAV09_3 and 1709_6 were analyzed at the University of Western Australia (UWA) by multi-collector inductively coupled plasma mass spectrometry (MC-ICPMS) using a NU Plasma II. Prior to analysis, samples were cleaned in H_2O_2 (for PTIMS) or in NaOCl (for MC-ICPMS) to remove organic material and then dissolved in HNO_3 , after which the boron was purified using ion chromatography. The boron separation technique used for the PTIMS is based on methodology by Wei et al. (2009) and refined by Trotter et al. (2011). For MC-ICPMS, a combined cation–anion ion-exchange technique was employed as described by McCulloch et al. (2014). In both methods, the boron is collected in relatively large fractions, ensuring 100 % collection efficiency. The $\delta^{11}\text{B}$ composition of water samples was analyzed by PTIMS following a simplified purification procedure (cf. coral samples) that omitted the H_2O_2 cleaning step and employed a single AGW50-X8 cation column elution followed by an IRA743 column elution (i.e., the final cation column was omitted). The amount of water sample required to extract and purify 1 μg of B was estimated from the relationship between the measured [B] and salinity (S) in the flood plume $\text{B} = 0.1299(S) + 0.1188$ and $\text{B} = 0.1302(S) - 0.0374$; 2007 and 2009, respectively (Fig. 2). The amount of water subjected to the boron extraction and purification procedure varied from 250 μL ($S = 35$) to 5000 μL ($S = 0.7$), while 30 000 μL was processed for the river water sample ($S = 0$).

All boron isotopic ratios are expressed in the conventional delta notation (δ) relative to the NBS951 boric acid international standard. Over the course of this study, PTIMS analysis of the SRM951 standard yielded a mean value of $\delta^{11}\text{B} = +0.05\text{‰}$ relative to a reference value for this standard of 4.054, with an external precision (2 SD) of $\pm 0.35\text{‰}$ ($n = 43$) and an internal precision of $\pm 0.07\text{‰}$. Repeated analyses of the samples ($n = 46$) gave an aver-

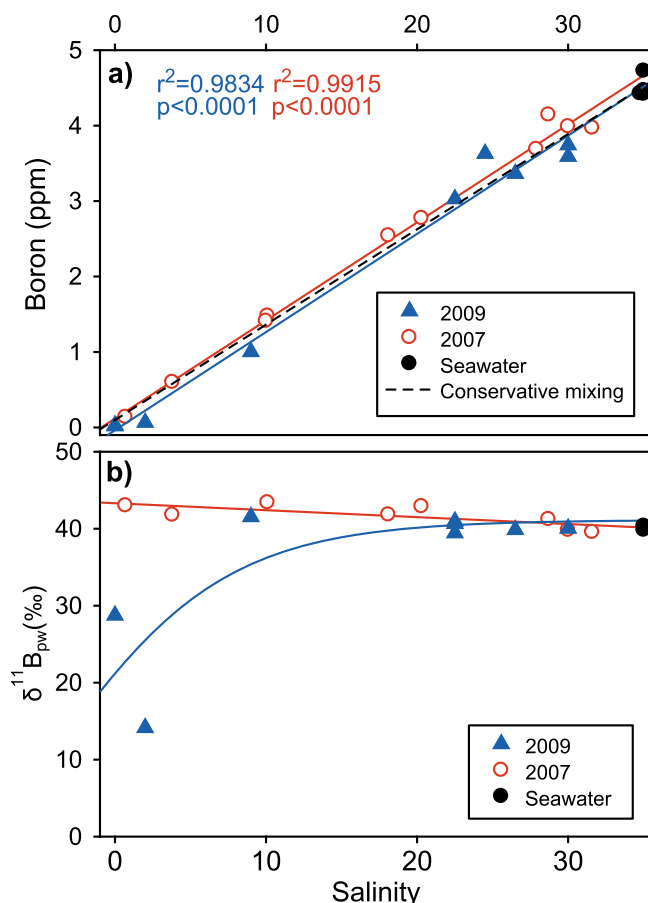


Figure 2. (a) Boron concentration plotted against salinity of waters from the flood events of 2007 and 2009. A linear regression through the data is compared to the theoretical conservative mixing relationship based on a seawater end member with 4.52 mg B / L at $S = 35$. (b) Boron isotope composition of waters along salinity transects from the 2007 and 2009 flood events.

age reproducibility of ± 0.20 ‰ (2 SD). A modern coral from Papua New Guinea (NEP B) was used as a secondary working standard. Repeated NEP B analyses gave an average value of 26.35 ± 0.44 ‰ (2 SD, $n = 33$) using PTIMS, and 25.96 ± 0.32 ‰ (2 SD, $n = 70$) using MC-ICPMS. The $\delta^{11}B_{carb}$ values of coral samples ($n = 8$) analyzed by PTIMS are consistently offset by $+0.45$ ‰ relative to the MC-ICPMS data. To maintain consistency between the two data sets, a $+0.45$ ‰ correction was therefore applied to the data measured by MC-ICPMS. Measurements of the international carbonate standards JCp-1 by MC-ICPMS gave a $\delta^{11}B$ value of 24.35 ± 0.34 ‰ (2 SD), identical to the 24.33 ± 0.11 ‰ (SE) reported by Foster et al. (2013) and 24.22 ± 0.28 ‰ (2 SD) reported by Wang et al. (2010).

Conversion of $\delta^{11}B_{carb}$ to pH of the calcifying fluid (pH_{cf}) values was undertaken using the relationship

$$pH_{cf} = pK_B - \log \left[\frac{\delta^{11}B_{sw} - \delta^{11}B_{carb}}{\alpha_{B3-B4} \times \delta^{11}B_{carb} - \delta^{11}B_{sw} + 1000(\alpha_{B3-B4} - 1)} \right], \quad (1)$$

where $\delta^{11}B_{sw}$ is the B isotope composition of seawater ($\delta^{11}B_{sw} = 39.61$ ‰; Foster et al., 2010) and the B isotope fractionation factor (α_{B3-B4}) of 1.0272 is taken from Klochko et al. (2006). The B dissociation constant (pK_B) was adjusted to the ambient temperature and salinity (Trotter et al., 2011), the latter especially relevant for corals from the inner-shelf reef region, which is diluted by fresh water during flood events. Seasonal variation in salinity was estimated based on the linear relationship observed between the magnitude of past flood events and corresponding salinity values reported by King et al. (2001) and Walker (1981) for these reefs (Supplement Fig. S1).

Average annual salinity values were estimated using the equation given in Fig. S1. For each year, a dilution factor derived from a 2-month period of maximum river discharge was applied to an initial seawater value of 35.5. Despite limitations with this approach, as flood events are spatially and temporally variable (King et al., 2001; Furnas, 2003), the effect after correcting the pK_B for salinity and temperature on the estimated pH_{sw} value is small ($< \sim 0.01$ pH units).

The external pH_{sw} value was estimated following the method for *Porites* sp. as described by Trotter et al. (2011):

$$pH_{sw} = (pH_{cf} - 5.954) / 0.32. \quad (2)$$

All measured and reconstructed pH_{sw} values are reported relative to the total pH scale.

3 Results

3.1 Plume waters boron concentration, $\delta^{11}B$ ratios, and pH during flood events

Measured [B] and $\delta^{11}B_{pw}$ are plotted against salinity of the water samples collected during the flood events of 2007 and 2009 (Fig. 2). Salinity ranges from 0 at the river mouth to 30 at Havannah Island and 26.5 at Pandora Reef. Salinity and [B] concentration during the flood events of 2007 and 2009 show a linear relationship ($r^2 = 0.9834$; $p < 0.0001$; $n = 10$ for 2007 and $r^2 = 0.9915$; $p < 0.0001$; $n = 8$ for 2009), consistent with conservative mixing of boron between seawater and floodwaters.

The flood events sampled in 2007 and 2009 show large differences in the $\delta^{11}B_{pw}$ composition of the low-salinity floodwaters collected close to the river mouth (Fig. 2). The low $\delta^{11}B_{pw}$ ($+14.13$ ‰) measured during the larger 2009 flood event (29 TL) contrasts with the less variable and higher $\delta^{11}B_{pw}$ ($+42.8$ ‰) of the smaller 2007 flood event (10 TL).

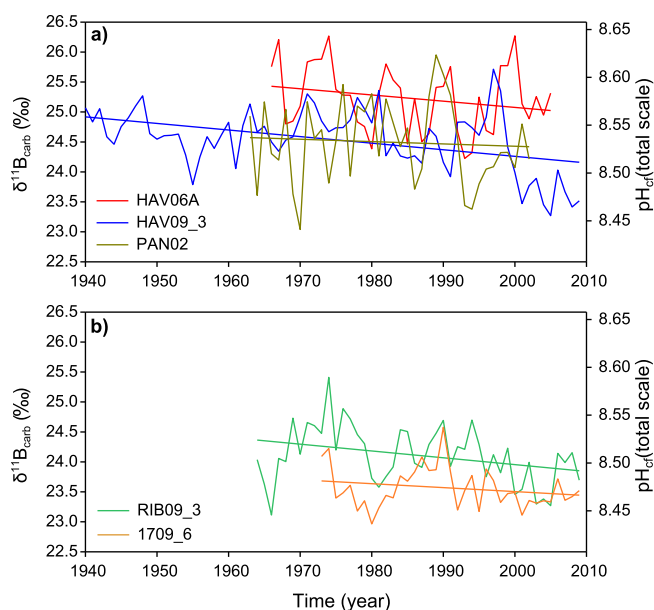


Figure 3. Annual time series and linear regressions for $\delta^{11}\text{B}_{\text{carb}}$ values and corresponding pH_{cf} of coral cores from (a) the inner-shelf reefs of Havannah Island and Pandora Reef, and (b) the mid-shelf reefs of Rib Reef and 17-065.

River water collected from the Burdekin River bridge (23 km upstream from the river mouth) during the 2009 flood event had a $\delta^{11}\text{B}_{\text{pw}}$ value of +28 ‰. Despite the large difference in the $\delta^{11}\text{B}_{\text{pw}}$ values of waters near the river mouth in the two flood events, $\delta^{11}\text{B}_{\text{pw}}$ of samples taken close to the inner-shelf reefs are very similar, with an average $\delta^{11}\text{B}$ value of 39.80 ± 0.34 ‰ (2 SD; $n = 2$). This value is identical to seawater samples from Lady Musgrave Island in the southern GBR ($\delta^{11}\text{B}_{\text{sw}} = 40.09 \pm 0.37$ ‰; 2 SD; $n = 2$), and is consistent with previously reported seawater values (Foster et al., 2010).

3.2 Coral $\delta^{11}\text{B}$ records

Coral $\delta^{11}\text{B}_{\text{carb}}$ compositions for five cores give average values that range from 23.6 ± 0.37 to 25.2 ± 0.57 ‰ over the common period of 1973 to 2002 (Table 2). These values are consistent with previously reported values for *Porites* corals (Hönisch et al., 2004; Pelejero et al., 2005; Wei et al., 2009; Krief et al., 2010). Using Eqs. (1) and (2), these $\delta^{11}\text{B}$ values translate to pH_{sw} values of 7.88 ± 0.07 to 8.19 ± 0.11 (Table 2). The mid-shelf corals have slightly lower $\delta^{11}\text{B}_{\text{carb}}$ (and pH) values that are less variable (± 0.37 to ± 0.44 ‰; 2 SD) than the inner-shelf corals (± 0.50 to ± 0.66 ‰; 2 SD). Differences in $\delta^{11}\text{B}_{\text{carb}}$ compositions between coral cores are significant (Kruskal–Wallis one-way ANOVA on ranks). Pairwise multiple comparison procedures (Tukey test; $p < 0.05$) indicate that these differences are significant between the three inner-shelf cores and the mid-shelf core 1709_6; mid-shelf core RIB09_3 is only significantly different from inner-

Table 1. Periods covered by coral core samples analyzed.

Region	Reef	Core	Years
Inner shelf	Havannah Is.	HAV06A	1966–2005
		HAV09_3	1940–2009
	Pandora	PAN02	1963–2002
Mid-shelf	Rib	RIB09_3	1964–2009
	17-065	1709_6	1973–2009

shelf core HAV06A. No significant correlation was found between the different $\delta^{11}\text{B}_{\text{carb}}$ coral records.

Linear regressions applied to the reconstructed annual pH_{sw} time series for all five coral records show a decrease in time over the full length of each coral records (Fig. 3). The decrease in pH_{sw} is equivalent to -0.017 ± 0.008 units per decade for the inner-shelf corals and -0.018 ± 0.007 units per decade for the mid-shelf corals. These rates are consistent with global estimates of 0.017 to 0.019 pH units decrease per decade from 1984 to 2011 based on instrumental data (Dore et al., 2009; Santana-Casiano et al., 2007; Bates et al., 2012), but are lower than the 0.041 ± 0.017 pH unit decrease per decade for the period of 1940 to 2004 shown by the $\delta^{11}\text{B}_{\text{carb}}$ coral records from Arlington Reef (mid-reef) in the central GBR previously reported by Wei et al. (2009). However, the Arlington Reef core exhibited a marked decrease in $\delta^{11}\text{B}_{\text{carb}}$ composition in association with the effects of the severe 1998 bleaching event.

Composite records for $\delta^{11}\text{B}_{\text{carb}}$ were obtained for the inner-shelf and mid-shelf corals (Fig. 4) for the periods of 1963 to 2005 and 1973 to 2009, respectively. These are the periods common to more than one core for each region. The data from each core were first normalized according to the following equation:

$$z_t = x_t - \bar{x}_c, \tag{3}$$

where x_t is a $\delta^{11}\text{B}_{\text{carb}}$ value at a certain point in time, \bar{x}_c is the mean $\delta^{11}\text{B}_{\text{carb}}$ value for a given coral. The composite records were then obtained by calculating the average from the normalized data at a certain point in time. To preserve the units, the composite records were “rescaled” according to the equation

$$r_t = \bar{Z}_t - \bar{x}_R, \tag{4}$$

where Z_t is a composite $\delta^{11}\text{B}_{\text{carb}}$ value at a certain point in time and \bar{x}_R is the average mean value for all the cores from a specific region. The $\delta^{11}\text{B}_{\text{carb}}$ annual composite for inner-shelf and mid-shelf records are plotted relative to time and compared with annual discharge from the Burdekin River, SST from HadISST1, and coral linear extension rates from D’Olivo et al. (2013; Fig. 4). The composite $\delta^{11}\text{B}_{\text{carb}}$ records for inner-shelf corals show significant correlation with river discharge, SST, and coral extension rates (Table 3). The mid-

Table 2. Average values and variability (2 SD) for coral $\delta^{11}\text{B}_{\text{carb}}$, pH_{cf} , and reconstructed pH_{sw} calculated over the common period of 1973–2002. The reconstructed pH_{sw} values were estimated using Eq. (2) to correct for the pH offset at the site of calcification. Slopes were obtained from the linear regression of the full length of each core (see Table 1) and are used to indicate the annual rate of change for the reconstructed pH_{sw} records. The uncertainty for the slopes is based on the external reproducibility for the standard.

	Core	$\delta^{11}\text{B}_{\text{carb}}$	pH_{cf}	pH_{sw}	
		Average	Average	Average	Slope (pH unit yr^{-1})
Inner shelf	HAV06A	25.17 ± 0.57	8.58 ± 0.04	8.19 ± 0.11	-0.0020 ± 0.0030
	HAV09_3	24.15 ± 0.50	8.54 ± 0.03	8.08 ± 0.10	-0.0023 ± 0.0011
	PAN02	24.54 ± 0.66	8.54 ± 0.04	8.07 ± 0.13	-0.0008 ± 0.0038
Mid-shelf	RIB09_3	24.20 ± 0.44	8.51 ± 0.03	8.00 ± 0.09	-0.0023 ± 0.0020
	1709_6	23.60 ± 0.37	8.48 ± 0.02	7.88 ± 0.07	-0.0013 ± 0.0021

Table 3. Pearson correlation coefficients (r) and corresponding p values for correlations of annual composite coral $\delta^{11}\text{B}_{\text{carb}}$ records from the inner shelf (1964–2005) and mid-shelf (1973–2009) with Burdekin River runoff, SST from HadISST1, and coral linear extension rates for the corresponding region taken from D'Olivo et al. (2013).

	River runoff (log ML)		SST ($^{\circ}\text{C}$)		Lin. ext. (cm yr^{-1})	
	r	p value	r	p value	r	p value
$\delta^{11}\text{B}_{\text{carb}}$ inner shelf ($n = 42$)	0.565	0.0001	-0.387	0.0103	-0.418	0.0053
$\delta^{11}\text{B}_{\text{carb}}$ mid-shelf ($n = 37$)	0.147	0.3860	-0.420	0.0096	-0.302	0.0733

shelf records shows a weaker but still significant correlation with SST.

The 8-year low-pass filter applied to the composite reconstructed pH_{sw} data derived from the three inner-shelf $\delta^{11}\text{B}_{\text{carb}}$ coral records reveals semi-decadal variation (Fig. 5), which is not observed in the mid-shelf $\delta^{11}\text{B}_{\text{carb}}$ data. Similar variability is observed in inner-shelf coral extension rates and calcification when periods of slower growth coincide with higher terrestrial runoff (D'Olivo et al., 2013). For inner-shelf corals it follows that higher $\delta^{11}\text{B}_{\text{carb}}$ (higher pH) signals coincide with periods of increased river discharge and slower extension rates.

4 Discussion

4.1 Variations in river and seawater $\delta^{11}\text{B}$ during flood events

The data from DERM (2011) show that the Burdekin River have an average pH_{rw} of 7.58 ± 0.46 (2 SD; Fig. S2); this indicates that low-pH fresh water, relative to pH_{sw} , is introduced into the coastal area of the GBR during wet periods. The pH_{rw} shows no significant difference between summer (7.56 ± 0.41 ; 2 SD) and winter (7.65 ± 0.35 ; 2 SD) values, with a decrease in pH during some high-discharge events, but there is no consistent seasonal pattern. The variability in pH_{rw} indicates that factors other than the amount of discharge or rainfall determine the pH_{rw} , and may reflect variability that is related to the nature of the material being car-

ried by the river and the catchment supplying the water. The $\delta^{11}\text{B}_{\text{pw}}$ near the mouth of the Burdekin River can vary significantly between different flood events (Fig. 2). Given that the $\delta^{11}\text{B}_{\text{rw}}$ is likely influenced by various factors, including both the type and amount of terrigenous material carried by the river during flood events as well as the source of the river runoff and nature of the catchment, more work is needed to characterize B dynamics and isotope fractionation mechanisms during flood events. Although the $\delta^{11}\text{B}_{\text{pw}}$ values during 2007 and 2009 show a large variation close to the Burdekin River mouth, the $\delta^{11}\text{B}_{\text{pw}}$ values near the inner-shelf reefs are typical of ocean waters (i.e., $\delta^{11}\text{B} \sim 40\text{‰}$).

4.2 Origin of interannual $\delta^{11}\text{B}_{\text{carb}}$ variability in corals

The results shown in Fig. 4 and corresponding correlations suggest a relationship between coral $\delta^{11}\text{B}_{\text{carb}}$ and both ambient seawater temperature and terrestrial runoff, particularly for the inner-shelf region of the GBR. However, the interannual pH_{sw} variability of less than ± 0.01 pH units, which is directly attributable to temperature and salinity changes due to river runoff, contrasts with the interannual variability of more than ± 0.07 pH units reconstructed from the $\delta^{11}\text{B}_{\text{carb}}$ compositions for the inner-shelf and mid-shelf corals. Possible explanations for the interannual variability observed in $\delta^{11}\text{B}_{\text{carb}}$ (reconstructed pH_{sw}) are examined below.

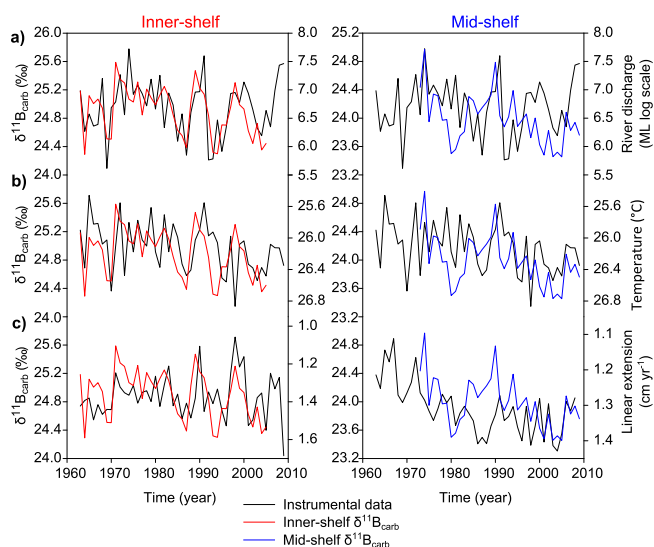


Figure 4. Annual composite $\delta^{11}\text{B}_{\text{carb}}$ records for the inner-shelf corals and mid-shelf corals compared to annual discharge from the Burdekin River (a), SST from HadISST1 (b), and coral linear extension rates from D'Olivo et al. (2013) for the corresponding inner-shelf or mid-shelf regions (c). Note that the temperature and linear extension axis has been reversed to facilitate comparisons.

4.2.1 Boron adsorption onto clays and sediments

The interannual $\delta^{11}\text{B}_{\text{carb}}$ variations for inner-shelf corals could be explained by the adsorption of B onto sediments and clays that are delivered to the inner-shelf region by rivers. Clays preferentially remove the lighter isotope ^{10}B from seawater (Palmer et al., 1987; Barth, 1998). This selective removal results in the respective depletion of ^{11}B in marine clays but enrichment in seawater, and is the accepted explanation for the heavy isotopic composition of seawater (e.g., 39.61 ± 0.04 ‰; Foster et al., 2010) relative to average continental crust (Spivack and Edmond, 1986; Palmer et al., 1987; Barth, 1998). Given the large silt and clay wash load transported from the Burdekin River (Belperio, 1979), fractionation of $\delta^{11}\text{B}$ between the dissolved and adsorbed B phases could have a significant effect on the $\delta^{11}\text{B}$ of seawater. However, the conservative mixing of B along the transect (Fig. 2) indicates that boron is not being quantitatively removed from the plume waters by clays, and that the clay material is already in equilibrium with the river water before entering the ocean. Similar results have been reported by Barth (1998) and Xiao et al. (2007). Furthermore, the oceanic $\delta^{11}\text{B}_{\text{pw}}$ values near the reefs during flood events and the low B concentration of river waters require that, at the reef sites, the $\delta^{11}\text{B}$ signal be dominated by seawater. Finally, large $\delta^{11}\text{B}_{\text{carb}}$ interannual variations occur on the mid-shelf reefs where there is no clay-dominated terrestrial runoff.

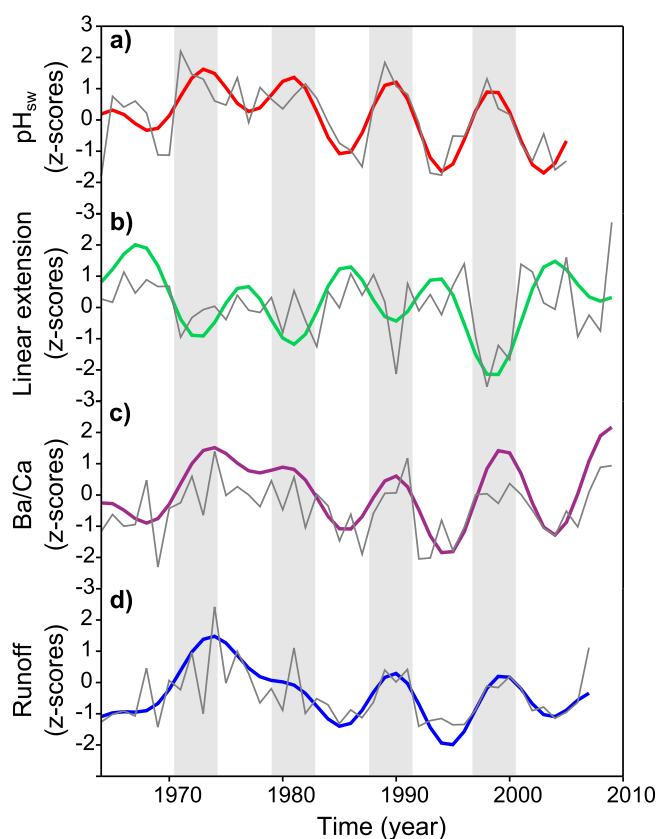


Figure 5. Normalized annual (grey) and smoothed (colored 8-year low-pass filter) time series for (a) the inner-shelf composite reconstructed pH_{sw} obtained from $\delta^{11}\text{B}_{\text{carb}}$ coral records, (b) averaged linear extension of inner shelf in the central GBR (D'Olivo et al., 2013), terrestrial influx indicated by (c) discharge from the Burdekin River, and (d) coral Ba/Ca data from Pandora and Havannah Island (McCulloch et al., 2003).

4.2.2 Effect of nutrient enrichment and biological productivity on pH_{sw}

River discharge is an important source of particulate and dissolved nutrients as well as sediments to the inner-shelf area of the GBR (King et al., 2002; Devlin and Brodie, 2005), being responsible for ~ 90 % of the particulate and dissolved nutrients introduced during flood events (Mitchell and Bramley, 1997; Furnas, 2003). Most particulate matter and sediments are deposited within a few kilometers (~ 10 km) of river mouths where salinity is < 10 (Wolanski and Jones, 1981), whereas dissolved nutrients are carried greater distances of up to ~ 200 km along the coast (Devlin and Brodie, 2005). Once the turbidity decreases and low light levels are no longer limiting, the dissolved nutrients are rapidly taken up by primary producers, resulting in phytoplankton blooms (Furnas, 2003; Devlin and Brodie, 2005; Brodie et al., 2010b). These blooms do not usually develop until the salinity reaches ~ 25 , typically between 50 and 200 km from

the river mouth (Devlin and Brodie, 2005), which is where the inner-shelf coral reefs of this study are located.

If we consider NO_3^- as the main form of nitrogen sourced from the Burdekin River into the inner-shelf area of the GBR (Furnas, 2003), plankton productivity will result in the decrease in seawater CO_2 , increase in alkalinity, and uptake of H^+ (Gattuso et al., 1999). The strong coupling between CO_2 dynamics and large phytoplankton bloom events observed at Kane'ohe Bay, Hawaii, changes the reef system from being a source of CO_2 to a sink of CO_2 (Drupp et al., 2011). At Kane'ohe Bay, bloom events are fueled by nutrient inputs following rainfall and terrestrial runoff events. The enhanced productivity is reflected by increased phytoplankton biomass from ~ 2 to $\sim 6 \mu\text{g L}^{-1}$ Chl *a*, which draws down $p\text{CO}_2$ by ~ 100 ppm (Drupp et al., 2011). Similar large nutrient-fueled changes in phytoplankton biomass occur in the central GBR, where Chl *a* increases from between 0.3 and $0.7 \mu\text{g L}^{-1}$ Chl *a* (Brodie et al., 2007) to up to $20 \mu\text{g L}^{-1}$ Chl *a* within flood plumes (Devlin and Brodie, 2005; Brodie et al., 2010a). For rivers in the central GBR, including the Burdekin, typical dissolved inorganic nitrogen (DIN) (chiefly NO_3^-) concentrations during flood conditions vary between 20 and $70 \mu\text{M}$, while dissolved inorganic phosphorus (DIP) varies between 0.15 and $1.3 \mu\text{M}$ (Furnas, 2003). These are much higher than typical seawater concentrations of $0.02 \mu\text{M}$ for DIP and $0.03 \mu\text{M}$ for NO_3^- during non-flood periods in the inshore region of the central GBR (Furnas et al., 2011).

The uptake of CO_2 from nutrient-enhanced productivity and the associated changes to the carbonate parameters during flood events in the central GBR were estimated using Redfield ratios and river flood plume nutrient loads (Fig. 6). For these calculations we assumed a conservative dilution process (Wooldridge et al., 2006). Three scenarios are included. In the first scenario only the changes due to the mixing of plume waters with seawater are considered (Fig. 6a). In the second scenario the input of nutrients from plume waters is included, with N assumed as the limiting nutrient (Fig. 6b). This scenario is consistent with observations that N appears to be the dominant control for new phytoplankton biomass formation in the GBR (Furnas et al., 2005). For the final scenario P is considered the limiting nutrient (Fig. 6c). When the effect of nutrient-enhanced productivity is not included (Fig. 6a), there is a small increase in pH_{sw} of up to 0.03 units under the most extreme flood conditions (e.g., salinity 24 near the reef). The scenarios with nutrient input from floodwaters in Fig. 6b and c result in a more marked increase in pH_{sw} due to the drawdown of $p\text{CO}_2$ associated with nutrient-enhanced productivity. In the case of the scenario with a salinity of 24 and DIN concentration of $23 \mu\text{M}$, there is a drawdown of $p\text{CO}_2$ of up to 300 ppm and a corresponding increase in pH_{sw} of ~ 0.33 units (Fig. 6b). It follows that the higher $\delta^{11}\text{B}_{\text{carb}}$ (and reconstructed pH_{sw}) values from the inner-shelf reefs during periods of high river discharge and high nutrient input are consistent with decreased $p\text{CO}_2$ and

increased pH_{sw} due to the stimulation of phytoplankton production.

In addition to the changes in pH_{sw} , there is a decrease in Ω_{arag} , under the flood scenario with no nutrient input (Fig. 6a), which is associated with the low TA and dissolved inorganic carbon (DIC) content of the floodwaters. The decrease in Ω_{arag} can be of up to 1 unit under extreme flood conditions (e.g., salinity 24). When nutrient-enhanced productivity is included, the negative effect from the plume waters on the Ω_{arag} is reduced (compare Fig. 6a with b and c) as the CO_2 uptake by the phytoplankton results in an increase in CO_3^{2-} .

Under the scenario with the highest DIN concentration ($23 \mu\text{M}$), the effect from the enhanced productivity is sufficient to counteract the dilution effect in Ω_{arag} , resulting in a net increase of up to 0.6 units (Fig. 6b). However, the reduction in Ω_{arag} that is expected under most flood conditions is likely to negatively affect coral calcification (McCulloch et al., 2012). One limitation for the present model is that it does not allow for air–sea equilibration, which is likely to reduce the effects from the enhanced productivity on the carbonate parameters.

4.2.3 Cross-shelf differences in coral $\delta^{11}\text{B}_{\text{carb}}$ and reconstructed pH_{sw}

A systematic cross-shelf pattern is observed in $\delta^{11}\text{B}_{\text{carb}}$ (and reconstructed pH_{sw}), with both average values and interannual variability being greater for inner-shelf corals compared to mid-shelf corals (Table 2). This cross-shelf pattern is consistent with the available, yet limited, pH_{sw} data that comprise summer (2007) values of 8.14 ± 0.003 (Gagliano et al., 2010) measured at Magnetic Island in the inner-shelf area, and summer 2012 values of 8.03 ± 0.03 measured at Davies Reef (Albright et al., 2013).

It is not surprising to find differences in reconstructed pH_{sw} values between reefs given that the GBR is characterized by significant spatial gradients in seawater parameters (e.g., temperature and water quality), especially across different shelfal environments (D'Olivo et al., 2013; Cantin and Lough, 2014; Fabricius et al., 2014). These spatial differences could, for example, account for the lower interannual variation of the coral $\delta^{11}\text{B}_{\text{carb}}$ records from the mid-shelf reefs compared to inner-shelf reefs through the decreased influence of river runoff on mid-shelf reefs as previously suggested by Wei et al. (2009).

The reason for the lack of correlation between the $\delta^{11}\text{B}_{\text{carb}}$ records at nearby reefs, specifically between Pandora and Havannah Island, is unclear. Differences in biologically driven effects (e.g., species or gender related) or local variability in environmental parameters (e.g., light regime) are possible explanations. Nevertheless, the overall good agreement between the composite $\delta^{11}\text{B}_{\text{carb}}$ coral records and the terrestrial runoff indices is encouraging, suggesting that multi-core replication (Lough, 2004; Jones et al., 2009) and consideration of ambient environmental conditions are es-

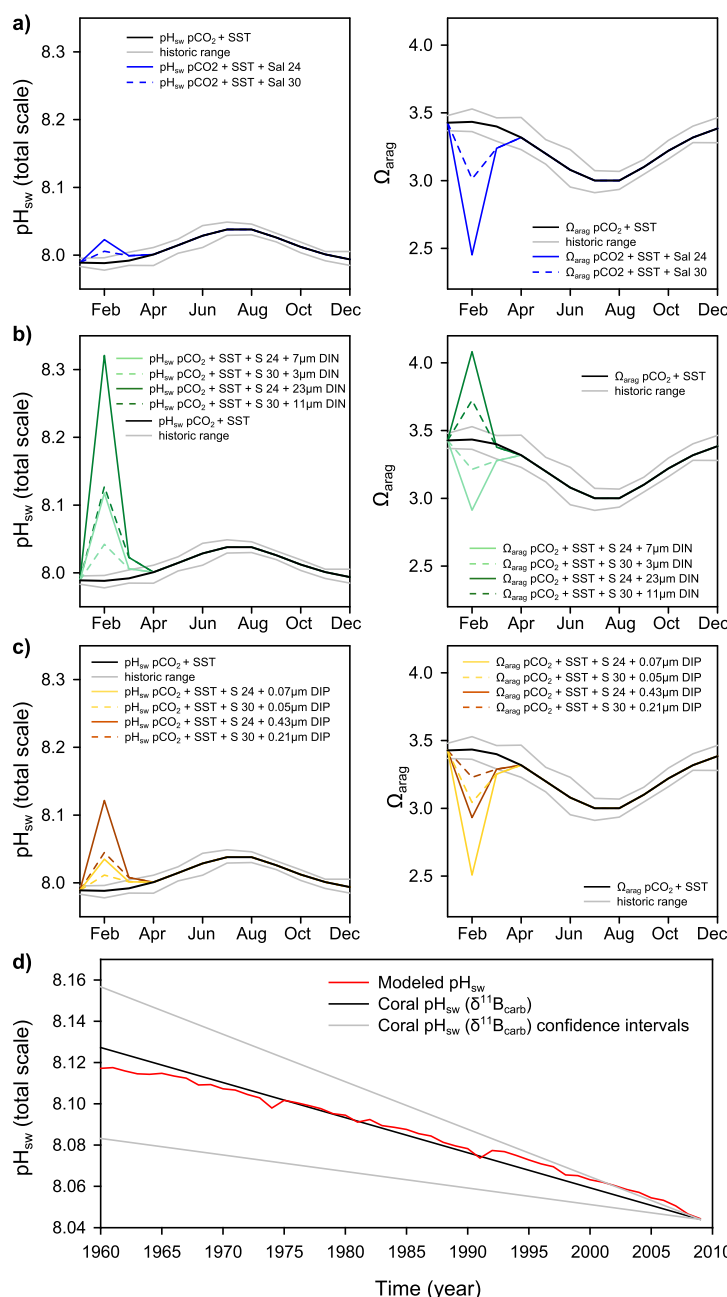


Figure 6. (a) Estimated seasonal pH_{sw} and Ω_{arag} changes based on in situ SST (AIMS, 2011) with an average pCO_2 of 431 ppm and a seasonal variation of 60 ppm (Uthicke et al., 2014). Seawater pH values were estimated considering a seawater end member with summer total alkalinity (TA) of 2270 mmol kg sw^{-1} and winter TA of 2256 mmol kg sw^{-1} (Uthicke et al., 2014); dissolved inorganic carbon (DIC) changes were estimated from TA and pCO_2 . The grey lines define the range of historic maximum and minimum SST values for any given month. Shown here are changes in pH_{sw} and Ω_{arag} resulting from a hypothetical flood event characterized by a decrease in salinity from 35 to values of 24 or 30 in February and increasing to 33 in March. For flood conditions the river water end member was estimated considering TA of 787.7 mmol kg sw^{-1} and DIC of 811.1 mmol kg sw^{-1} (DERM, 2014). (b) Estimated seasonal pH_{sw} and Ω_{arag} changes as in (a), including DIC changes associated with the CO_2 drawdown due to enhanced phytoplankton production during flood events based on DIN river inputs of 20 and 70 μM in February and assuming conservative dilution. Nutrient inputs are estimated to reduce by half in March and back to seawater levels by April. (c) Estimated seasonal pH_{sw} and Ω_{arag} changes as in (b) considering DIP river inputs of 0.15 and 1.3 μM in February and assuming conservative dilution. (d) Estimated annual pH_{sw} changes with time based on reconstructed SST (HadISST1), changes in atmospheric CO_2 (NOAA), and salinity changes associated with flood events obtained from the equation in Fig. S1. A comparison based on the average pH_{sw} slope obtained from all the coral $\delta^{11}B_{carb}$ data in Table 2 is included. The minimum and maximum slopes obtained for the corals in Table 2 are included as confidence intervals. Calculations were made using CO_2SYS with carbonate constants K1 and K2 from Merzbach et al. (1973) refitted by Dickson and Millero (1987), and for sulfate from Dickson (1990) with 0 dbar pressure.

sential when interpreting $\delta^{11}\text{B}_{\text{carb}}$ records. Further analyses of additional records from the same area should help clarify the uncertainties and improve our understanding of the $\delta^{11}\text{B}_{\text{carb}}$ seawater proxy in dynamic reefal systems that characterize inshore environments. A multi-proxy approach should also prove helpful in confirming the results from this study, as well as determining the response of corals to specific environmental parameters such as SST, nutrients, sediment, or pH_{sw} .

4.2.4 Relationship between $\delta^{11}\text{B}_{\text{carb}}$ (reconstructed pH_{sw}) and coral growth rates

Calcification and linear extension rates of inner-shelf corals from the GBR show a long-term decrease from the period of 1930 to 2008 (Lough, 2008; D'Olivo et al., 2013). The decrease in coral growth has been attributed to factors ranging from thermal stress, bleaching, eutrophication, and ocean acidification (Cooper et al., 2008; Lough, 2008; De'ath et al., 2009; D'Olivo et al., 2013). The present study reveals that decadal-scale wet periods with increased terrestrial runoff in the central GBR coincide with periods of reduced inner-shelf coral growth (Fig. 5). The decrease in coral growth occurs despite higher ambient pH_{sw} , as determined from $\delta^{11}\text{B}_{\text{carb}}$. Given the apparently more favorable pH_{sw} for coral growth during wet periods, other factors such as degraded water quality or reduced Ω_{arag} must clearly be responsible for the decline in extension rates observed during wet periods. For example, nutrient-fueled increase in phytoplankton biomass has been a longstanding explanation for the drowning of coral reefs throughout the geological records (Hallock and Schlager, 1986). More in situ monitoring of seawater carbonate system parameters (e.g., Uthicke et al., 2014), especially during wet periods, would greatly help in understanding the response of the complex inner-shelf systems to changes in water quality.

4.2.5 Physiological controls on coral calcification

The coral pH_{cf} values calculated from the measured $\delta^{11}\text{B}_{\text{carb}}$ compositions (Table 2) indicate that corals elevate the pH at the site of calcification, in agreement with previous studies (Al-Horani et al., 2003; Venn et al., 2011; McCulloch et al., 2012). This elevation of pH_{cf} for massive *Porites* grown in the natural environment is estimated to be 0.41 ± 0.02 for the inner-shelf corals and 0.43 ± 0.03 for the mid-shelf corals. The latter values were estimated using the coral pH_{cf} values in Table 2 and the directly measured pH_{sw} summer value of 8.14 from Gagliano et al. (2010) as an independent reference value for the inner-shelf region, and an average pH_{sw} annual value of 8.06 from Albright et al. (2013) for the mid-shelf region.

Aside from pH up-regulation at the calcification site (McCulloch et al., 2012), other processes involved in promoting aragonite precipitation include the transport of ions to

the mineralization site and the synthesis of an organic matrix (Allemand et al., 2004; Venn et al., 2011). Inhibition or reduced activity of these processes has been associated with significant reduction of calcification in other studies (Tambutte et al., 1996; Allemand et al., 1998, 2004; Al-Horani et al., 2003). The reduction in growth of inner-shelf coral may thus be explained by the effects of river discharge that likely include a decrease in Ω_{arag} that is accompanied by an increase in shading, turbidity, sedimentation, or competition for carbon from the photosynthetic activity of zooxanthellae. These factors can affect the availability of DIC, enzyme activity, or synthesis of the organic matrix involved in the calcification process (Tambutte et al., 1996; Allemand et al., 1998, 2004; Al-Horani et al., 2003), because energy and DIC required by these processes is reallocated into cleaning or mucus production (Riegl and Branch, 1995; Telesnicki and Goldberg, 1995; Philipp and Fabricius, 2003). Therefore, it should not be surprising to find reduced growth during wet periods and hence degraded water quality despite conditions of higher pH. Critically, this demonstrates the overriding importance of local reef-water quality relative to the subordinate longer-term effects of ocean acidification.

In contrast to the inner-shelf reefs, the $\delta^{11}\text{B}_{\text{carb}}$ records of the mid-shelf corals shows no significant relationship to river discharge, consistent with the reduced effects of river flood plumes. Extreme flood events can, however, occasionally reach the mid-shelf reefs, especially when offshore winds occur (King et al., 2002). The presence of subdued luminescent bands in coral records from Rib Reef that coincide with some large river discharge events confirms the minor effect of flood events in the mid-shelf region. Nevertheless, coral linear extension and calcification at both mid- and outer-shelf reefs increase over the last ~ 50 years, coincident with the rise in temperature over this period (D'Olivo et al., 2013). This observed increase in coral calcification, despite the decrease in the reconstructed pH_{sw} , indicates that ocean acidification has so far played a secondary role in impacting coral calcification in the mid-shelf region.

5 Summary and conclusions

Coral $\delta^{11}\text{B}_{\text{carb}}$ values show cross-shelf variability with higher average and amplitude values characteristic of the corals closer to the coast. The reconstructed pH_{sw} values calculated from the coral $\delta^{11}\text{B}_{\text{carb}}$ indicate that, in their natural environment, massive *Porites* up-regulate pH_{cf} by ~ 0.4 units. Variability in coral $\delta^{11}\text{B}_{\text{carb}}$ shows an interannual range in reconstructed pH_{sw} from ~ 0.07 pH units in mid-shelf corals to ~ 0.11 pH units in inner-shelf corals, compared to a much smaller long-term (1940 to 2009) trend of ~ 0.017 pH unit decrease per decade. This rate of change is consistent with previous estimates of decreasing surface pH_{sw} from pCO_2 -driven ocean acidification. Results from $\delta^{11}\text{B}_{\text{carb}}$ and coral growth indicate that terrestrial runoff has a significant

effect on inner-shelf reef environments. We propose that phytoplankton blooms, fueled by increased nutrient inputs from river plume waters, drive the drawdown of dissolved CO₂ and thus increase the pH in surface seawaters. Consequently, on a local scale the inner-shelf reefs of the GBR exhibit high rates of nutrient-driven production, and following river discharge events temporarily counter the effects of ocean acidification. Despite the higher pH_{sw}, we observe an associated decrease in coral linear extension and calcification (D'Olivo et al., 2013), consistent with expectations of a coral calcification decrease with decreasing Ω_{arag} (McCulloch et al., 2012). The incompatible relationship of higher pH_{sw} and decreased coral growth suggests that the effects of large flood events on lowering Ω_{arag} and degrading water quality (e.g., increased shading, turbidity, sedimentation, or competition for carbon by up-regulated photosynthetic activity of zooxanthellae) are the dominant cause of reduced coral growth. This study demonstrates the value of coral $\delta^{11}\text{B}$ as a paleo-proxy for reconstructing past pH_{sw} changes, as well as the importance of disentangling the effects of changing local water quality from ocean acidification and global warming, which is relevant not only to the inner-shelf region of the GBR but also other coral systems worldwide.

The Supplement related to this article is available online at doi:10.5194/bg-12-1223-2015-supplement.

Acknowledgements. The authors are grateful for financial support from the Australian Research Council Centre of Excellence for Coral Reef Studies provided to M. T. McCulloch and J. P. D'Olivo. M. T. McCulloch was also supported by a Western Australian Premier's Fellowship and an ARC Laureate Fellowship. J. P. D'Olivo was also supported by a PhD scholarship from the Research School of Earth Science, Australian National University. The research was completed while J. P. D'Olivo was holding a research associate position at UWA funded by NERP Tropical Ecosystems Hub Project 1.3 awarded to M. T. McCulloch. We thank Stephen Lewis (James Cook University), who collected (2007) and assisted (2009) with the collection of water samples and kindly provided the salinity data for water samples. G. Mortimer provided support for the $\delta^{11}\text{B}$ measurements at ANU. We thank J. Falter, S. A. Aciego, and one anonymous referee for their constructive comments on the manuscript.

Edited by: D. Gillikin

References

Albright, R., Langdon, C., and Anthony, K. R. N.: Dynamics of seawater carbonate chemistry, production, and calcification of a coral reef flat, central Great Barrier Reef, *Biogeosciences*, 10, 6747–6758, doi:10.5194/bg-10-6747-2013, 2013.

- Al-Horani, F. A., Al-Moghrabi, S. M., and de Beer, D.: The mechanism of calcification and its relation to photosynthesis and respiration in the scleractinian coral *Galaxea fascicularis*, *Mar. Biol.*, 142, 419–426, 2003.
- Allemand, D., Tambutt, E. E., Girard, J. P., and Jaubert, J.: Organic matrix synthesis in the scleractinian coral *Stylophora pistillata*: role in biomineralization and potential target of the organotin tributyltin, *J. Exp. Biol.*, 201, 2001–2009, 1998.
- Allemand, D., Ferrier-Pages, C., Furla, P., Houlbrequé, F., Puverel, S., Reynaud, S., Tambutte, E., Tambutte, S., and Zoccola, D.: Biomineralisation in reef-building corals: from molecular mechanisms to environmental control, *C. R. Palevol.*, 3, 453–467, 2004.
- Andersson, A. J., Mackenzie, F. T., and Lerman, A.: Coastal ocean and carbonate systems in the high CO₂ world of the anthropocene, *Am. J. Sci.*, 305, 875–918, 2005.
- Barth, S.: ¹¹B / ¹⁰B variations of dissolved boron in a freshwater-seawater mixing plume (Elbe Estuary, North Sea), *Mar. Chem.*, 62, 1–14, 1998.
- Bates, N. R., Amat, A., and Andersson, A. J.: Feedbacks and responses of coral calcification on the Bermuda reef system to seasonal changes in biological processes and ocean acidification, *Biogeosciences*, 7, 2509–2530, doi:10.5194/bg-7-2509-2010, 2010.
- Bates, N. R., Best, M. H. P., Neely, K., Garley, R., Dickson, A. G., and Johnson, R. J.: Detecting anthropogenic carbon dioxide uptake and ocean acidification in the North Atlantic Ocean, *Biogeosciences*, 9, 2509–2522, doi:10.5194/bg-9-2509-2012, 2012.
- Belperio, A.: The combined use of wash loads and bed material load rating curves for the calculation of total load: an example from the Burdekin River, Australia, *Catena*, 6, 317–329, 1979.
- Brodie, J., Fabricius, K., De'ath, G., and Okaji, K.: Are increased nutrient inputs responsible for more outbreaks of crown-of-thorns starfish? An appraisal of the evidence, *Mar. Pollut. Bull.*, 51, 266–278, 2005.
- Brodie, J. E., De'ath, G., Devlin, M., Furnas, M., and Wright, M.: Spatial and temporal patterns of near-surface chlorophyll a in the Great Barrier Reef lagoon, *Mar. Freshwater Res.*, 58, 342–353, 2007.
- Brodie, J. E., Schroeder, T., Rohde, K., Faithful, J., Masters, B., Dekker, A., Brando, V., and Maughan, M.: Dispersal of suspended sediments and nutrients in the Great Barrier Reef lagoon during river-discharge events: conclusions from satellite remote sensing and concurrent flood-plume sampling, *Mar. Freshwater Res.*, 61, 651–664, 2010a.
- Brodie, J. E., Devlin, M., Haynes, D., and Waterhouse, J.: Assessment of the eutrophication status of the Great Barrier Reef lagoon (Australia), *Biogeochemistry*, 106, 281–302, 2010b.
- Brodie, J. E., Wolanski, E., Lewis, S., and Bainbridge, Z.: An assessment of residence times of land-sourced contaminants in the Great Barrier Reef lagoon and the implications for management and reef recovery, *Mar. Pollut. Bull.*, 65, 267–279, 2012.
- Cantin, N. E. and Lough, J. M.: Surviving coral bleaching events: *Porites* growth anomalies on the Great Barrier Reef, *PLoS ONE*, 9, e88720, doi:10.1371/journal.pone.0088720, 2014.
- Cooper, T. F., De'Ath, G., Fabricius, K. E., and Lough, J. M.: Declining coral calcification in massive *Porites* in two nearshore regions of the northern Great Barrier Reef, *Glob. Change Biol.*, 14, 529–538, 2008.

- D'Olivo, J. P., McCulloch, M. T., and Judd, K.: Long-term records of coral calcification across the central Great Barrier Reef: assessing the impacts of river runoff and climate change, *Coral Reefs*, 32, doi:10.1007/s00338-013-1071-8, 2013.
- De'ath, G. and Fabricius, K.: Water quality as a regional driver of coral biodiversity and macroalgae on the Great Barrier Reef, *Ecol. Appl.*, 20, 840–850, 2010.
- De'ath, G., Lough, J. M., and Fabricius, K. E.: Declining coral calcification on the Great Barrier Reef, *Science*, 323, 116–119, 2009.
- Devlin, M. J. and Brodie, J.: Terrestrial discharge into the Great Barrier Reef Lagoon: nutrient behavior in coastal waters, *Mar. Pollut. Bull.*, 51, 9–22, 2005.
- Dickson, A. G.: Thermodynamics of the dissociation of boric acid in synthetic seawater from 273.15 to 318.15 K, *Deep-Sea Res.*, 37, 755–766, 1990.
- Dickson, A. G. and Millero, F. J.: A Comparison of the Equilibrium Constants for the Dissociation of Carbonic-Acid in Seawater Media, *Deep-Sea Res.*, 34, 1733–1743, 1987.
- Doney, S. C., Fabry, V. J., Feely, R. A., and Kleypas, J. A.: Ocean acidification: the other CO₂ problem, *Ann. Rev. Mar. Sci.*, 1, 169–192, 2009.
- Dore, J. E., Lukas, R., Sadler, D. W., Church, M. J., and Karl, D. M.: Physical and biogeochemical modulation of ocean acidification in the central North Pacific, *P. Natl. Acad. Sci. USA*, 106, 12235–12240, 2009.
- Drupp, P., De Carlo, E. H., Mackenzie, F. T., Bienfang, P., and Sabine, C. L.: Nutrient Inputs, Phytoplankton Response, and CO₂ Variations in a Semi-Enclosed Subtropical Embayment, Kaneohe Bay, Hawaii, *Aquat. Geochem.*, 17, 473–498, 2011.
- Duarte, C. M., Hendriks, I. E., Moore, T. S., Olsen, Y. S., Steckbauer, A., Ramajo, L., Carstensen, J., Trotter, J. A., and McCulloch, M.: Is Ocean Acidification an Open-Ocean Syndrome? Understanding Anthropogenic Impacts on Seawater pH, *Estuar. Coasts*, 36, 221–236, 2013.
- Fabricius, K. E., Logan, M., Weeks, S., and Brodie, J.: The effects of river run-off on water clarity across the central Great Barrier Reef, *Mar. Pollut. Bull.*, 84, 191–200, doi:10.1016/j.marpolbul.2014.05.012, 2014.
- Falter, J. L., Lowe, R. J., Zhang, Z., and McCulloch, M.: Physical and biological controls on the carbonate chemistry of coral reef waters: effects of metabolism, wave forcing, sea level, and geomorphology, *PLoS ONE*, 8, e53303, doi:10.1371/journal.pone.0053303, 2013.
- Foster, G. L., Pogge von Strandmann, P. A. E., and Rae, J. W. B.: Boron and magnesium isotopic composition of seawater, *Geochim. Geophys. Geosys.*, 11, Q08015, doi:10.1029/2010gc003201, 2010.
- Foster, G. L., Hönisch, B., Paris, G., Dwyer, G. S., Rae, J. W. B., Elliott, T., Gaillardet, J., Hemming, N. G., Louvat, P., and Vengosh, A.: Interlaboratory comparison of boron isotope analyses of boric acid, seawater and marine CaCO₃ by MC-ICPMS and NTIMS, *Chem. Geol.* 358, 1–14, 2013.
- Frithsen, J. B., Keller, A. A., and Pilson, M. E. Q.: Effects of inorganic nutrient additions in coastal areas: a mesocosm experiment; data report, Marine Ecosystems Research Laboratory, Graduate School of Oceanography, University of Rhode Island, 1985.
- Furnas, M.: Catchments and corals: terrestrial runoff to the Great Barrier Reef, Australian Institute of Marine Science and Reef CRC, Townsville, Australia, 2003.
- Furnas, M., Mitchell, A., Skuza, M., and Brodie, J.: In the other 90 %: phytoplankton responses to enhanced nutrient availability in the Great Barrier Reef Lagoon, *Mar. Pollut. Bull.*, 51, 253–265, 2005.
- Furnas, M., Alongi, D., McKinnon, D., Trott, L., and Skuza, M.: Regional-scale nitrogen and phosphorus budgets for the northern (14°S) and central (17° S) Great Barrier Reef shelf ecosystem, *Continent. Shelf Res.*, 31, 1967–1990, 2011.
- Gagliano, M., McCormick, M. I., Moore, J. A., and Depczynski, M.: The basics of acidification: baseline variability of pH on Australian coral reefs, *Mar. Biol.*, 157, 1849–1856, 2010.
- Gattuso, J.-P., Frankignoulle, M., and Smith, S. V.: Measurement of community metabolism and significance in the coral reef CO₂ source-sink debate, *P. Natl. Acad. Sci. USA*, 96, 13017–13022, 1999.
- Hallock, P. and Schlager, W.: Nutrient excess and the demise of coral reefs and carbonate platforms, *PALAIOS*, 1, 389–398, 1986.
- Hemming, N. G. and Hanson, G. N.: Boron isotopic composition and concentration in modern marine carbonates, *Geochim. Cosmochim. Ac.*, 56, 537–543, 1992.
- Hinga, K. R.: Effects of pH on coastal marine phytoplankton, *Mar. Ecol.-Prog. Ser.*, 238, 281–300, 2002.
- Hönisch, B., Hemming, N. G., Grottoli, A. G., Amat, A., Hanson, G. N., and Buma, J.: Assessing scleractinian corals as recorders for paleo-pH: Empirical calibration and vital effects, *Geochim. Cosmochim. Ac.*, 68, 3675–3685, 2004.
- Jones, P. D., Briffa, K. R., Osborn, T., Lough, J., van Ommen, T. D., Vinther, B. M., Luterbacher, J., Wahl, E. R., Zwiers, F. W., Mann, M. E., Schmidt, G. A., Ammann, C. M., Buckley, B. M., Cobb, K. M., Esper, J., Goosse, H., Graham, N., Jansen, E., Kiefer, T., Kull, C., Küttel, E., Mosley-Thompson, E., Overpeck, J. T., Riedwyl, N., Schultz, M., Tudhope, A. W., Villalba, R., Wanner, H., Wolff, E., and Xoplaki, E.: High-resolution palaeoclimatology of the last millennium: a review of current status and future prospects, *Holocene*, 19, 3–49, 2009.
- King, B., McAllister, F., Wolanski, E., Done, T., and Spagnol, S.: River plume dynamics in the central Great Barrier Reef, in: *Oceanographic Processes of Coral reefs: Physical and Biological Links in the Great Barrier Reef*, edited by: Wolanski, E., CRC Press, Boca Raton, 145–160, 2001.
- King, B., McAllister, F., and Done, T.: Modelling the impact of the Burdekin, Herbert, Tully and Johnstone River plumes on the Central Great Barrier Reef, CRC Reef Research Centre, Townsville44, 2002.
- Kleypas, J. A.: Geochemical Consequences of Increased Atmospheric Carbon Dioxide on Coral Reefs, *Science*, 284, 118–120, 1999.
- Klochko, K., Kaufman, A. J., Yao, W., Byrne, R. H., and Tossell, J. A.: Experimental measurement of boron isotope fractionation in seawater, *Earth Planet. Sc. Lett.*, 248, 276–285, 2006.
- Krief, S., Hendy, E. J., Fine, M., Yam, R., Meibom, A., Foster, G. L., and Shemesh, A.: Physiological and isotopic responses of scleractinian corals to ocean acidification, *Geochim. Cosmochim. Ac.*, 74, 4988–5001, 2010.

- Lewis, S. E., Shields, G. A., Kamber, B. S., and Lough, J. M.: A multi-trace element coral records of land-use changes in the Burdekin River catchment, NE Australia, *Palaeogeogr. Palaeoclimatol.*, 246, 471–487, 2007.
- Liu, Y., Liu, W., Peng, Z., Xiao, Y., Wei, G., Sun, W., He, J., Liu, G., and Chou, C.-L.: Instability of seawater pH in the South China Sea during the mid-late Holocene: Evidence from boron isotopic composition of corals, *Geochim. Cosmochim. Acta.*, 73, 1264–1272, 2009.
- Lough, J.: Climate variability and change on the Great Barrier Reef, in: *Oceanographic Processes of Coral Reefs: Physical and Biological Links in the Great Barrier Reef*, edited by: Wolanski, E., CRC Press, Boca Raton, Florida, 269–300, 2001.
- Lough, J. M.: A strategy to improve the contribution of coral data to high-resolution paleoclimatology, *Palaeogeogr. Palaeoclimatol.*, 204, 115–143, 2004.
- Lough, J. M.: Tropical river flow and rainfall reconstructions from coral luminescence: Great Barrier Reef, Australia, *Paleoceanography*, 22, PA2218, doi:10.1029/2006pa001377, 2007.
- Lough, J. M.: Coral calcification from skeletal records revisited, *Mar. Ecol.-Prog. Ser.*, 373, 257–264, 2008.
- Lough, J. M.: Measured coral luminescence as a freshwater proxy: comparison with visual indices and a potential age artefact, *Coral Reefs*, 30, 169–182, 2011.
- McCulloch, M., Falter, J., Trotter, J., and Montagna, P.: Coral resilience to ocean acidification and global warming through pH up-regulation, *Nat. Clim. Change*, 2, 623–627, 2012.
- McCulloch, M. T., Fallon, S., Wyndham, T., Hendy, E., Lough, J. M., and Barnes, D. J.: Coral records of increased sediment flux to the inner Great Barrier Reef since European settlement, *Nature*, 421, 727–730, 2003.
- McCulloch, M. T., Holcomb, M., Rankenburg, K., and Trotter, J. A.: Rapid, high-precision measurements of boron isotopic compositions in marine carbonates, *Rapid. Commun. Mass. Spectrom.*, 28, 2704–2712, 2014.
- Merzbach, C., Culberson, C. H., Hawley, J. E., and Pytkowicz, R. M.: Measurement of the apparent dissociation constants of carbonic acid in seawater at atmospheric pressure, *Limnol. Oceanogr.*, 18, 897–907, 1973.
- Mitchell, A. W. and Bramley, R. G. V.: Export of nutrients and suspended sediment from the Herbert river catchment during a flood event associated with cyclone Sadie, *Cyclone Sadie Flood Plumes in the GBR lagoon: Composition and Consequences*, Workshop series, Great Barrier Reef Marine Park Authority, No. 22, 1997.
- Palmer, M. R., Spivack, A. J., and Edmond, J. M.: Temperature and pH controls over isotopic fractionation during adsorption of boron on marine clay, *Geochim. Cosmochim. Acta.*, 51, 2139–2323, 1987.
- Pelejero, C., Calvo, E., McCulloch, M. T., Marshall, J. F., Gagan, M. K., Lough, J. M., and Opdyke, B. N.: Preindustrial to modern interdecadal variability in coral reef pH, *Science*, 309, 2204–2207, 2005.
- Philipp, E. and Fabricius, K.: Photophysiological stress in scleractinian corals in response to short-term sedimentation, *J. Exp. Mar. Biol. Ecol.*, 287, 57–78, 2003.
- Reynaud, S., Hemming, N. G., Juillet-Leclerc, A., and Gattuso, J. P.: Effect of ρCO_2 and temperature on the boron isotopic composition of the zooxanthellate coral *Acropora* sp, *Coral Reefs*, 23, 539–546, 2004.
- Riegl, B. and Branch, G. M.: Effects of sediment on the energy budgets of four scleractinian (Bourne 1900) and five alcyonacean (Lamouroux 1816) corals, *J. Exp. Mar. Biol. Ecol.*, 186, 259–275, 1995.
- Salisbury, J., Green, M., Hunt, C., and Campbell, J.: Coastal acidification by rivers: a threat to shellfish?, *EOS*, 89, 513–528, 2008.
- Santana-Casiano, J. M., González-Dávila, M., Rueda, M.-J., Llinás, O., and González-Dávila, E.-F.: The interannual variability of oceanic CO₂ parameters in the northeast Atlantic subtropical gyre at the ESTOC site, *Global Biogeochem. Cy*, 21, GB1015, doi:10.1029/2006gb002788, 2007.
- Shinjo, R., Asami, R., Huang, K.-F., You, C.-F., and Iryu, Y.: Ocean acidification trend in the tropical North Pacific since the mid-20th century reconstructed from a coral archive, *Mar. Geol.*, 342, 58–64, doi:10.1016/j.margeo.2013.06.002, 2013.
- Simpson, J. J. and Zirino, A.: Biological-control of pH in the Peruvian coastal upwelling area, *Deep-Sea Res.*, 27, 733–744, 1980.
- Spivack, A. J. and Edmond, J. M.: Determination of boron isotope ratios by thermal ionization mass-spectrometry of the dicesium metaborate cation, *Anal. Chem.*, 58, 31–35, 1986.
- Sweatman, H., Delean, S., and Syms, C.: Assessing loss of coral cover on Australia's Great Barrier Reef over two decades, with implications for longer-term trends, *Coral Reefs*, 30, 521–531, 2011.
- Tambutte, E., Allemand, D., Mueller, E., and Jaubert, J.: A compartmental approach to the mechanism of calcification in hermatypic corals, *J. Exp. Biol.*, 199, 1029–1041, 1996.
- Telesnicki, G. J. and Goldberg, W. M.: Effects of turbidity on the photosynthesis and respiration of two south Florida Reef coral species, *B Mar. Sci.*, 57, 527–539, 1995.
- Trotter, J., Montagna, P., McCulloch, M., Silenzi, S., Reynaud, S., Mortimer, G., Martin, S., Ferrier-Pagès, C., Gattuso, J.-P., and Rodolfo-Metalpa, R.: Quantifying the pH 'vital effect' in the temperate zooxanthellate coral *Cladocora caespitosa*: Validation of the boron seawater pH proxy, *Earth Planet. Sc. Lett.*, 303, 163–173, 2011.
- Uthicke, S., Furnas, M., and Lonborg, C.: Coral reefs on the edge?, Carbon chemistry on inshore reefs of the great barrier reef, *PLoS one*, 9, e109092, doi:10.1371/journal.pone.0109092, 2014.
- Vengosh, A., Kolodny, Y., Starinsky, A., Chivas, A. R., and McCulloch, M. T.: Coprecipitation and Isotopic Fractionation of Boron in Modern Biogenic Carbonates, *Geochim. Cosmochim. Acta.*, 55, 2901–2910, 1991.
- Venn, A., Tambutte, E., Holcomb, M., Allemand, D., and Tambutte, S.: Live tissue imaging shows reef corals elevate pH under their calcifying tissue relative to seawater, *PLoS ONE*, 6, e20013, doi:10.1371/journal.pone.0020013, 2011.
- Walker, T.: Seasonal Salinity Variations in Cleveland Bay, Northern Queensland, *Aust. J. Mar. Fresh. Res.*, 32, 143–149, 1981.
- Wang, B. S., You, C. F., Huang, K. F., Wu, S. F., Aggarwal, S. K., Chung, C. H., and Lin, P. Y.: Direct separation of boron from Na- and Ca-rich matrices by sublimation for stable isotope measurement by MC-ICP-MS, *Talanta*, 82, 1378–1384, 2010.
- Wei, G., McCulloch, M. T., Mortimer, G., Deng, W., and Xie, L.: Evidence for ocean acidification in the Great Barrier Reef of Australia, *Geochim. Cosmochim. Acta.*, 73, 2332–2346, 2009.

Wolanski, E. and Jones, M.: Physical properties of the Great Barrier Reef lagoon waters near Townsville. I effects of Burdekin River floods, *Aust. J. Mar. Fresh. Res.*, 32, 305–319, 1981.

Xiao, Y., Liao, B., Wang, Z., Wei, H., and Zhao, Z.: Isotopic composition of dissolved boron and its geochemical behavior in a freshwater-seawater mixture at the estuary of the Changjiang (Yangtze) River, *Chinese J. Geochem.*, 26, 105–113, 2007.